

Equivalent mutual inductance model for underwater wireless power transfer

Weiting Zhang , Jiateng Jiang , Wangqiang Niu *

Key Laboratory of Transport Industry of Marine Technology and Control Engineering,
Shanghai Maritime University, Shanghai, China
Corresponding author* : wqniu@shmtu.edu.cn

Abstract:

The circuit model in air of the wireless power transfer (WPT) systems is no longer applicable in seawater because of underwater eddy current loss (ECL). By analyzing the influence of seawater, it is considered that seawater mainly affects the self-inductance and mutual inductance of coils. Thus, the equivalent mutual inductance model of underwater WPT is established. It was verified by an experimental WPT system with an outer diameter of 22.5 cm and a resonant frequency of 470 kHz. The experimental results show that the output of the model is consistent with the measured results, and the model can be used to describe the underwater WPT system.

Key Word: underwater WPT system; equivalent mutual inductance; circuit model.

Date of Submission: 28-03-2022

Date of Acceptance: 09-04-2022

I. Introduction

In today's era of limited resources, wireless power transfer (WPT) systems with no direct physical contact, getting rid of the bondage of the wire, high flexibility, can work under strict and special condition. WPT systems have a wide range of applications in scientific research, medical treatment, entertainment, travel, communication and other aspects [1-4]. For underwater environment, WPT systems also have a wide range of applications, such as underwater robot, and underwater autonomous vehicles [5-7].

At present, there are many researches on transmission characteristics of underwater WPT systems. Eddy current loss is an important issue. [8] studied the influencing factors of eddy current loss in seawater by numerical method, and pointed out that smaller current, lower operating frequency, smaller transmission distance and smaller number of turns would lead to smaller eddy current loss. [9] made an in-depth study of the energy transmission mechanism and eddy current loss in seawater by using the principle of magnetic coupling resonance, and found that with the increase of working frequency, eddy current loss first increases and then decreases. The approximate formula for calculating eddy current loss is obtained, which shows that the eddy current loss of seawater clearance is proportional to the quadratic power of resonant frequency, the quadratic power of transmission coil radius, and the quadratic power of magnetic inductance intensity.

In order to study the performance of underwater WPT systems, circuit models are used widely. Studying the electric field intensity of each point in air and seawater, and analyzing the size of ECL in seawater, an improved model of underwater WPT system is proposed in [10], that is, an ECL resistor is introduced into two coils respectively. By adding compensation inductance in the primary circuit, the system has the same resonant frequency in air and seawater, which improves the transmission efficiency of the systems. A WPT systems model suitable for seawater is established. [11] derived a coupled circuit model with equivalent eddy current loss impedance from the three-coil model. The eddy current loss impedance is independent of coil distance, but proportional to operating frequency.

Frequency splitting is another critical issue. [12] systematically studied the frequency splitting phenomenon in series tuned contactless power transmission system in air by circuit theory. However, in another study [13], it was found that the phenomenon of frequency splitting disappeared in seawater. The reason for the disappearance of high frequency flat ridge was given in the paper as large eddy current loss in water, but there was no more systematic explanation.

In this paper, an equivalent mutual inductance model for underwater WPT systems is established to describe above experimental results. This paper is divided into four parts. The first part introduces the previous research results. The circuit model is established in the second part. The third part carries on the experiment verification. Finally, the fourth part gives conclusions.

II. Underwater WPT System Circuit Model

The basic circuit model of a bilaterally symmetric WPT system in air is shown in Fig. 1. In order to simplify the model and analysis, the series-series topology is chosen in this paper. Where, the leftmost circuit is the primary side, and the rightmost is the secondary side; U is the excitation voltage source; I_1 is the primary current; R_1 , C_1 and L_1 are the primary resistance, capacitance, and inductance, respectively; I_2 is the secondary current; C_2 and L_2 are the secondary capacitance, and inductance, respectively; M is the mutual inductance between the two coils; R_L is the secondary load resistance; R_{p1} is the internal resistance of primary coil, and capacitor; and R_{p2} is the internal resistance of secondary coil, and capacitor.

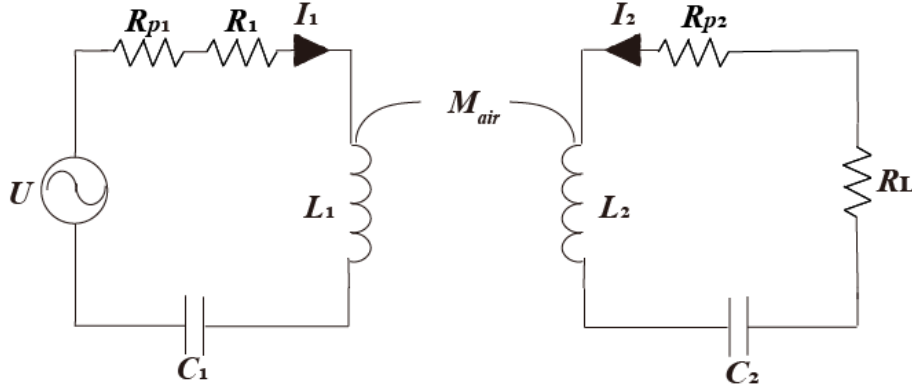


Fig. 1 Circuit model of bilaterally symmetric WPT system in air.

In general, the internal resistances R_{p1} and R_{p2} are small, and can be ignored in calculation. In the following formula, the letter marked and capitalized is vector, and the lowercase letters are effective values of corresponding vectors.

The loop equations are

$$\begin{aligned} \dot{U} &= R_1 \dot{I}_1 + j\omega L_1 \dot{I}_1 - j \frac{1}{\omega C_1} \dot{I}_1 - j\omega M \dot{I}_2 \\ 0 &= R_2 \dot{I}_2 + j\omega L_2 \dot{I}_2 - j \frac{1}{\omega C_2} \dot{I}_2 - j\omega M \dot{I}_1 \end{aligned} \quad (1)$$

Cancel out I_1 , then

$$j\omega M \dot{U} = \left[\left(R_1 + j\omega L_1 - j \frac{1}{\omega C_1} \right) \left(R_2 + j\omega L_2 - j \frac{1}{\omega C_2} \right) + (\omega M)^2 \right] \dot{I}_2 \quad (2)$$

Let

$$a = \left(R_1 + j\omega L_1 - j \frac{1}{\omega C_1} \right) \left(R_2 + j\omega L_2 - j \frac{1}{\omega C_2} \right) = h + jg \quad (3)$$

Where, h is the real part of the product of the total impedance of the primary side and the total impedance of the secondary side. And g is the imaginary part of the product of the total impedance of the primary side and the total impedance of the secondary side.

From (3), the formula (2) becomes

$$j\omega M \dot{U} = [a + (\omega M)^2] \dot{I}_2 \quad (4)$$

Take the effective value of both sides of equation (4), then

$$\omega M u = \sqrt{[h + (\omega M)^2]^2 + g^2} i_2 \quad (5)$$

That is

$$\omega^4 M^4 + \left[2h - \left(\frac{u}{i_2} \right)^2 \right] \omega^2 M^2 + h^2 + g^2 = 0 \quad (6)$$

Mutual inductance M can be obtained by solving equation (6).

Eddy current loss is considered generally the main reason for the difference in the transmission effect of WPT system in air and seawater. The coil consists of two parts, one is self-inductance and the other is mutual inductance, so these two parts can be used as variables to establish the underwater WPT system model, Fig. 2.

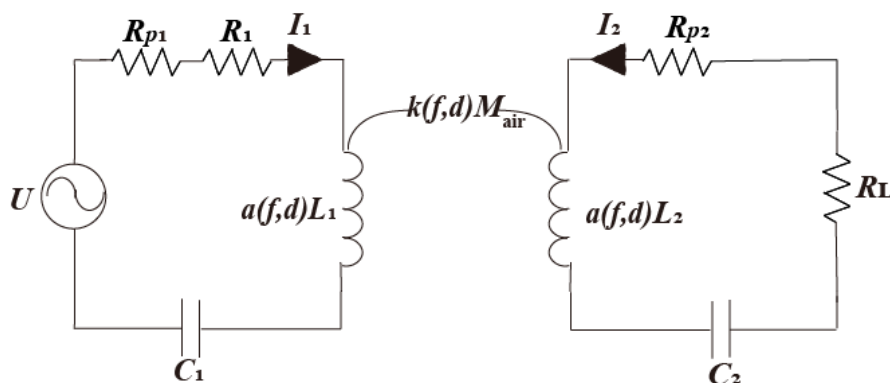


Fig. 2 Equivalent circuit model of underwater WPT system.

Where, k is the ratio of mutual inductance of the two coils in seawater and air; a is the ratio of self-inductance of the two coils in seawater and air. The model in this study is a symmetrical circuit, so the self-inductance ratio of the two coils is same, which is a . Since the main influencing factors of WPT system are the transfer distance d between the two coils and the working frequency f , it is considered that the two ratios k and a are dependent on the transfer distance and the working frequency.

III. Experimental Section

Compared with ordinary solenoid coils, planar spiral coils have the characteristics of magnetic field concentration and strong anti-offset ability [14]. Therefore, they are adopted in this study. The experiment coils are shown in Fig. 3, the coil is a plane coil wound with AWG16 wire of 17 turns, the inner diameter of the coil is 12 cm, and the outer diameter is 22.5 cm. Put it into a 120×70×70 cm tank with a water depth of 65 cm, and 19.6 kg of salt is melted to make the seawater salinity reach 3.5%. The underwater WPT experimental platform is shown in Fig. 4 [13]. The test parameters are shown in Table 1.

The sinusoidal wave output by the signal generator (Tektronix: AFG3102) is amplified by a 10 W power amplifier (Rigol: PA1011). The sinusoidal wave with a peak-peak value of 20 V is used as the input power to access the line.

The peak-to-peak values of the voltage on both sides of the required components are measured through the oscilloscope (Rigol: DS1302). The frequency range is 240-700 kHz, and a set of data is measured at intervals of 10 kHz. The distance between the two coils is 27-527 mm.

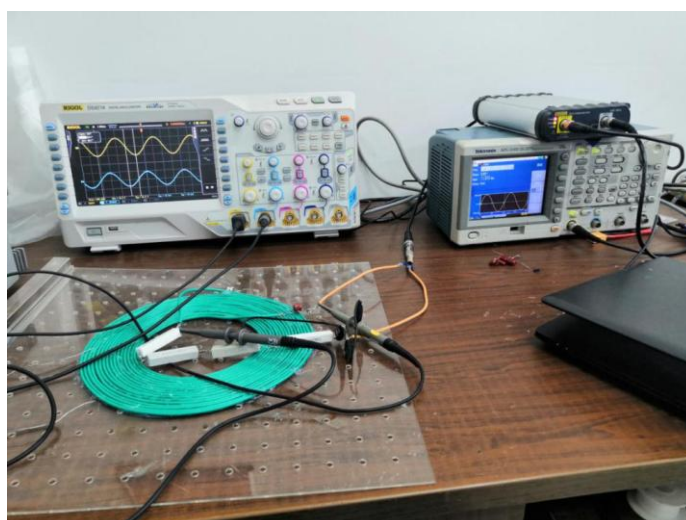


Fig. 3 Experiment coil of WPT systems.



Fig. 4 Underwater WPT system experimental platform.

Table 1: Test parameters

parameter	value
L_1	73.4 μ H
C_1	1.6 nF
R_1	44.2 ohm
R_{p1}	1.1 ohm
f_{01}	470 kHz
L_2	70.4 μ H
C_2	1.6 nF
R_L	44.7 ohm
R_{p2}	0.5 ohm
f_{02}	470 kHz

f_{01} and f_{02} are the resonant frequencies of primary side and secondary side respectively.

Measurement of output voltage in air

Put the two coils in air, connect the circuits according to the experimental circuit diagram, change the working frequency of the input voltage and the distance between the two coils. Measure and record the voltage of the secondary side load resistance. Fig. 5 shows the measured result.

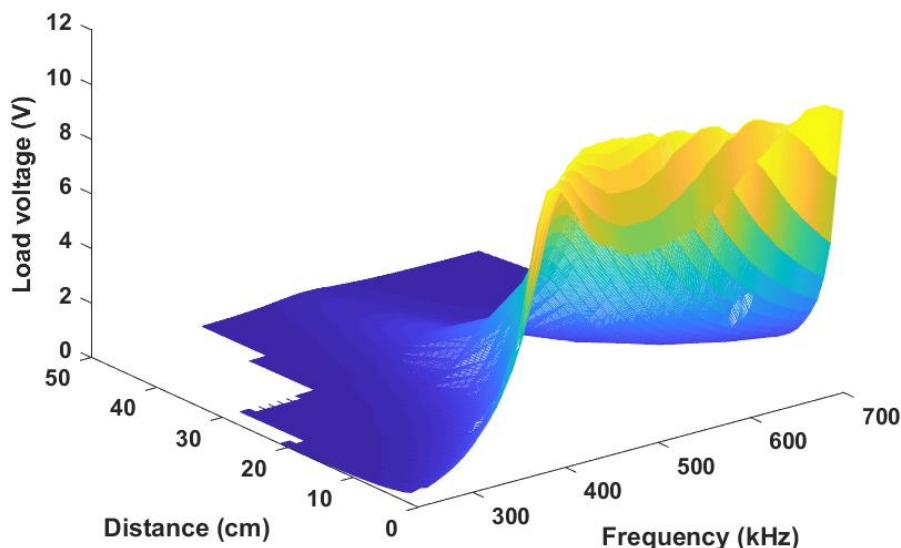


Fig. 5 3D diagram of measured secondary load voltage in air.

Measurement of output voltage in seawater

Put the two coils in seawater, connect the circuits according to the experimental circuit diagram, change the working frequency of the input voltage and the distance between the two coils. Measure and record the voltage of the secondary side load resistance. Fig. 6 shows the measured result.

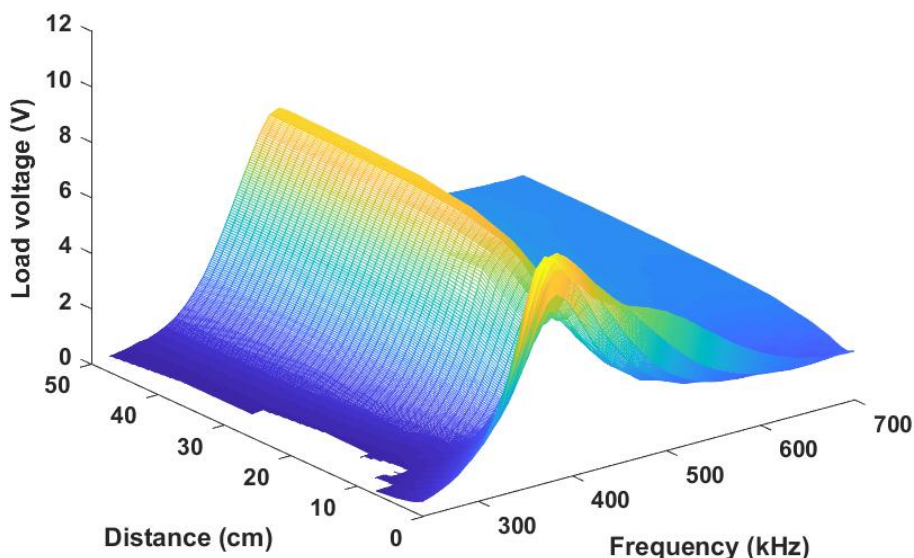


Fig. 6 3D diagram of measured secondary load voltage in seawater.

Experimental results

It can be seen from Fig. 5&6 that the transfer characteristics of WPT system in air and seawater is very different. One is that when the transfer distance is small, there is the frequency splitting phenomenon in air; the other is that when the transfer distance is large, the secondary side load voltage in seawater is much higher than that in air.

It can be seen from Fig. 7 that the resonant frequency of the WPT system in this experiment is 470 kHz in air, but shifts to left in seawater, and the peak-to-peak value of the load voltage frequently appears near 440 kHz. Therefore, the resonant frequency in seawater is considered to be 440 kHz, so the self-inductance of the coils is constant, that is, the ratio a is a constant. It can be calculated that the underwater self-inductance changes to 81.8 μ H.

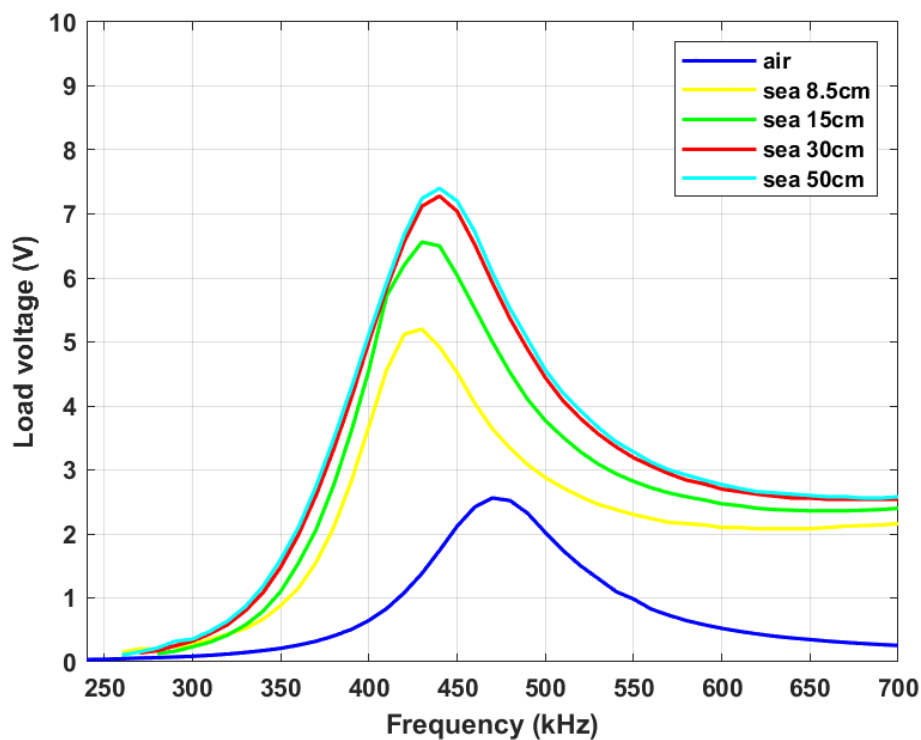


Fig. 7 Resonant frequency shift.

Based on the changed self-inductance, the mutual inductance in seawater can be calculated by the method introduced in the second part, as shown in Fig. 8.

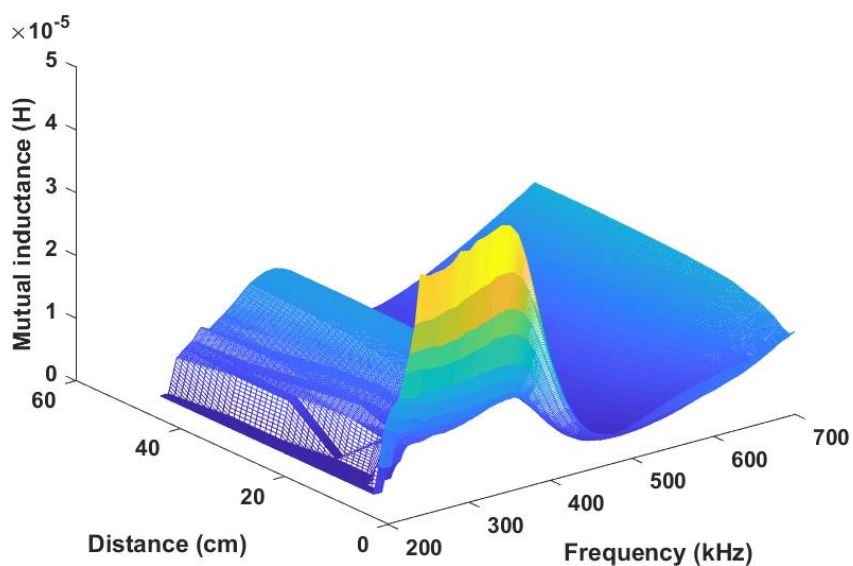


Fig. 8 Mutual inductance value

From (7), the mutual inductance ratio of WPT system in seawater and air is shown in Fig. 9.

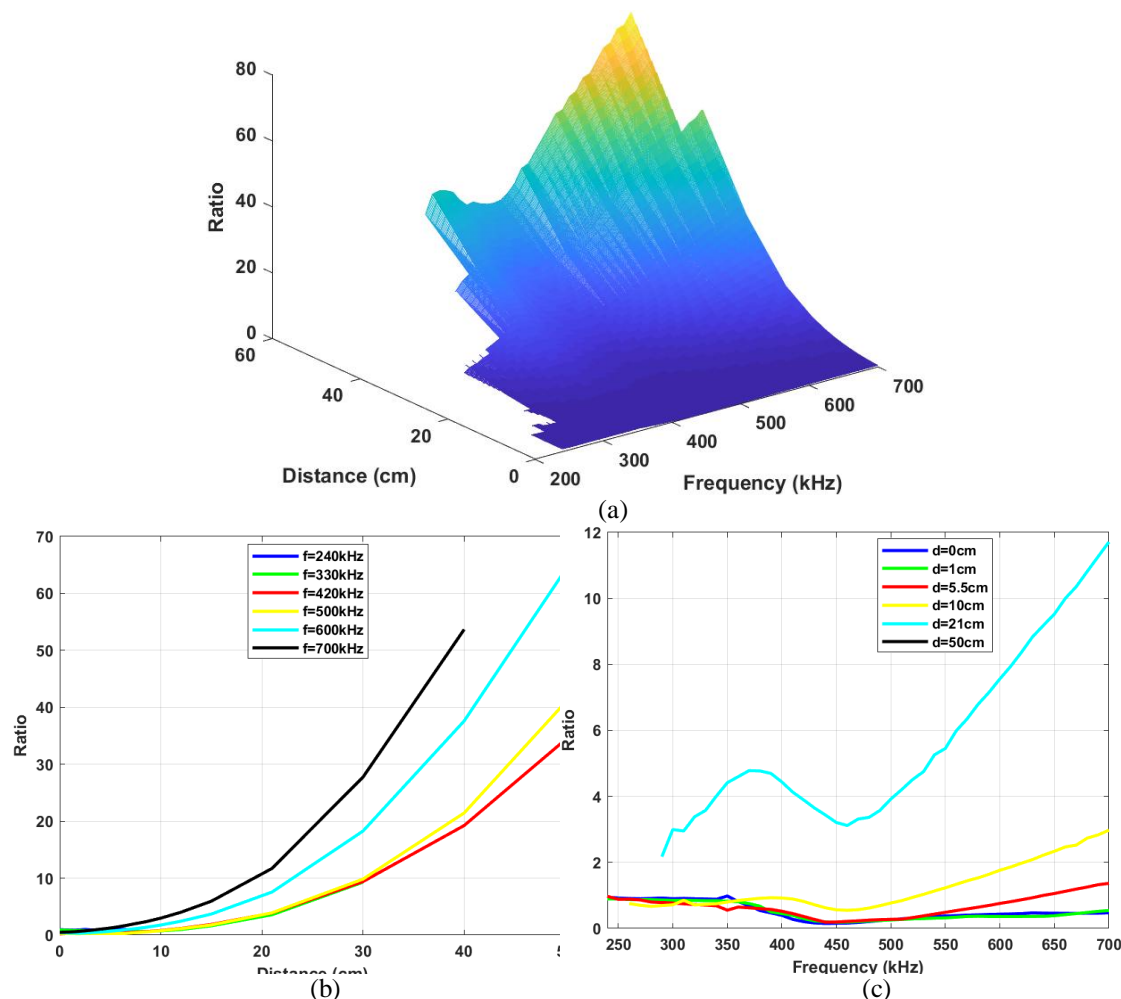


Fig. 9 The mutual inductance ratio of WPT system in seawater and air. (a) 3D diagram; (b) Relationship with distance; (c) Relationship with frequency

It can be seen from Fig. 9a that when the distance is small and the frequency is low, the ratio k of mutual inductance between seawater and air is nearly 1, so the mutual inductance between air and seawater is basically the same. As the distance increases and the frequency increases, the ratio becomes larger, that is, the mutual inductance in seawater is much larger than that in air. The frequencies of 240 kHz to 700 kHz are divided into three sections, 240 kHz to 380 kHz as low frequency, 390 kHz to 440 kHz as middle frequency, and 450 kHz to 700 kHz as high frequency. It can be seen from Fig. 9b that the ratio k of mutual inductance between seawater and air is always proportional to the cubic power of distance. According to Fig. 9c, the relationship between ratio and frequency is as follows: proportional at low frequency, inversely proportional at medium frequency, and proportional at high frequency.

The ratio is fitted by above relationship, as shown in Fig. 10.

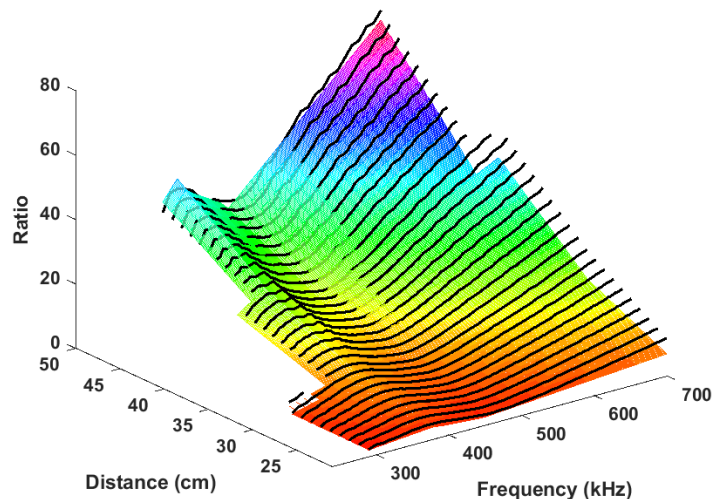


Fig. 10 3D diagram of the mutual inductance ratio. The black lines are measured data and the colorful surface is the theoretical values.

Model validation

Fig. 11 shows the three-dimensional comparison between theoretical mutual inductance calculated by the circuit model and experimental data; Fig. 12 shows the three-dimensional comparison between theoretical load voltage and experimental data.

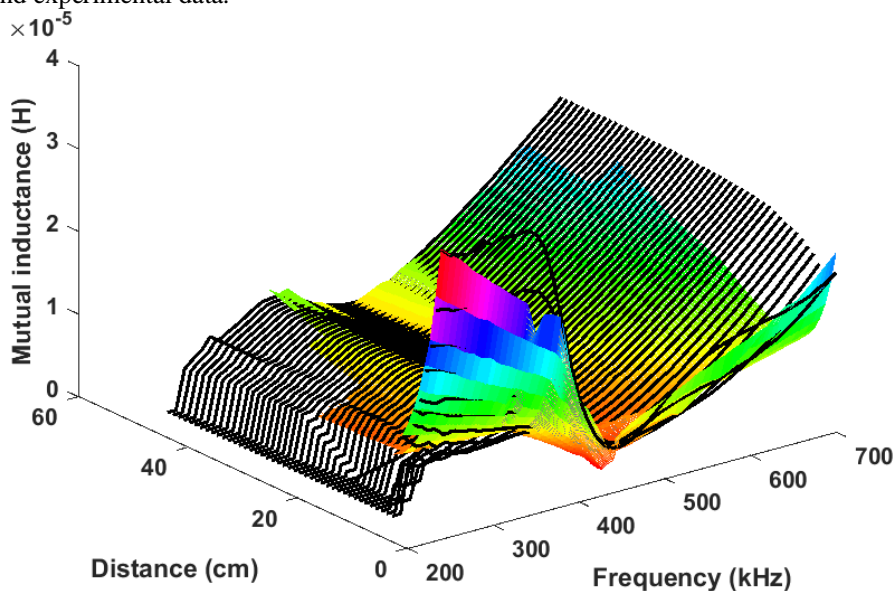


Fig. 11 3D diagram of the underwater mutual inductance. The black lines are measured data and the colorful surface is the theoretical values.

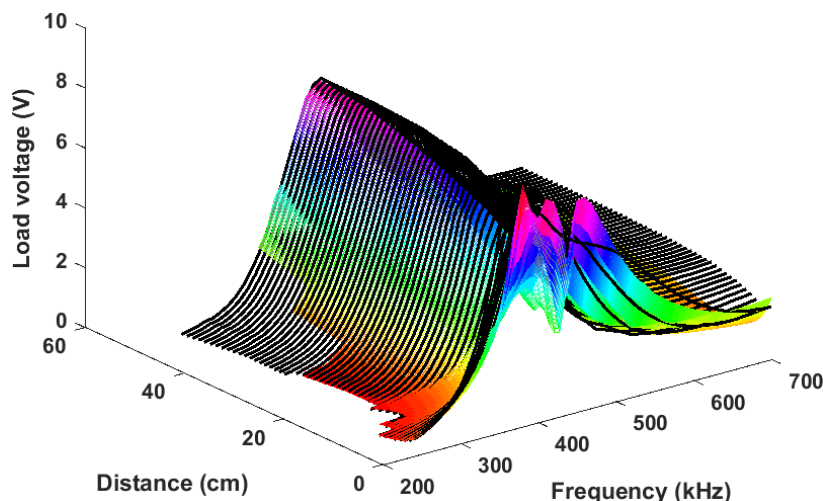


Fig. 12 3D diagram of secondary load voltage in seawater. The red lines are measured data and the colorful surface is the theoretical values.

Fig. 11&12 shows that the output results of the model are basically consistent with the experimental measurement results.

IV. Conclusions

This paper presents a variable mutual inductance circuit model of underwater WPT system. The calculated results of this model consist with the experimental results, so the model can describe and predict the transfer characteristics of underwater WPT system. It is worth mentioning that in the experiment of this study, it is found that the WPT system with the resonant frequency of 470 kHz, and when the transmission distance is greater than a certain value, the transfer efficiency of seawater is much higher than that of air, which should be further explored in the future.

References

- [1]. S. Y. Chu, X. Cui, X. Zan and A. -T. Avestruz, "Transfer-Power Measurement Using a Non-Contact Method for Fair and Accurate Metering of Wireless Power Transfer in Electric Vehicles," in *IEEE Transactions on Power Electronics*, vol. 37, no. 2, pp. 1244-1271, Feb. 2022, doi: 10.1109/TPEL.2021.3105689.
- [2]. J. Pries, V. P. N. Galigekere, O. C. Onar and G. Su, "A 50-kW Three-Phase Wireless Power Transfer System Using Bipolar Windings and Series Resonant Networks for Rotating Magnetic Fields," in *IEEE Transactions on Power Electronics*, vol. 35, no. 5, pp. 4500-4517, May 2020, doi: 10.1109/TPEL.2019.2942065.
- [3]. B. Luo, T. Long, L. Guo, R. Dai, R. Mai and Z. He, "Analysis and Design of Inductive and Capacitive Hybrid Wireless Power Transfer System for Railway Application," in *IEEE Transactions on Industry Applications*, vol. 56, no. 3, pp. 3034-3042, May-June 2020, doi: 10.1109/TIA.2020.2979110.
- [4]. Y. Jiang, L. Wang, J. Fang, R. Li, R. Han and Y. Wang, "A High-Efficiency ZVS Wireless Power Transfer System for Electric Vehicle Charging With Variable Angle Phase Shift Control," in *IEEE Journal of Emerging and Selected Topics in Power Electronics*, vol. 9, no. 2, pp. 2356-2372, April 2021, doi: 10.1109/JESTPE.2020.2984575.
- [5]. Z. Yan, B. Song, Y. Zhang, K. Zhang, Z. Mao and Y. Hu, "A Rotation-Free Wireless Power Transfer System With Stable Output Power and Efficiency for Autonomous Underwater Vehicles," in *IEEE Transactions on Power Electronics*, vol. 34, no. 5, pp. 4005-4008, May 2019, doi: 10.1109/TPEL.2018.2871316.
- [6]. T. Kan, R. Mai, P. P. Mercier and C. C. Mi, "Design and Analysis of a Three-Phase Wireless Charging System for Lightweight Autonomous Underwater Vehicles," in *IEEE Transactions on Power Electronics*, vol. 33, no. 8, pp. 6622-6632, Aug. 2018, doi: 10.1109/TPEL.2017.2757015.
- [7]. C. Cai, Y. Zhang, S. Wu, J. Liu, Z. Zhang and L. Jiang, "A Circumferential Coupled Dipole-Coil Magnetic Coupler for Autonomous Underwater Vehicles Wireless Charging Applications," in *IEEE Access*, vol. 8, pp. 65432-65442, 2020, doi: 10.1109/ACCESS.2020.2984530.
- [8]. Zhou J, Li D J and Chen Y, "Frequency selection of an inductive contactless power transmission system for ocean observing," in *Ocean Engineering*, vol. 60, no. 3, pp. 175-185, 2013.
- [9]. K. Zhang, L. Yan, Z. Yan, H. Wen and B. Song, "Modeling and analysis of eddy-current loss of underwater contact-less power transmission system based on magnetic coupled resonance," *Acta Physica Sinica*, vol. 65, no. 4, pp. 334-342, 2016.
- [10]. K. Zhang, Y. Ma, Z. Yan, Z. Di, B. Song and A. P. Hu, "Eddy current loss and detuning effect of seawater on wireless power transfer," in *IEEE Journal of Emerging and Selected Topics in Power Electronics*, vol. 8, DOI 10.1109/JESTPE.2018.2888521, no. 1, pp. 909-917, March 2020.
- [11]. W. Niu, C. Ye and W. Gu, "Circuit coupling model containing equivalent eddy current loss impedance for wireless power transfer in seawater," in *International Journal of Circuits, Systems and Signal Processing*, vol. 15, DOI 10.46300/9106.2021.15.45, pp. 410-416, 2021.
- [12]. W. Niu, J. Chu, W. Gu and A. Shen, "Exact Analysis of Frequency Splitting Phenomena of Contactless Power Transfer Systems," in *IEEE Transactions on Circuits and Systems I: Regular Papers*, vol. 60, no. 6, pp. 1670-1677, June 2013, doi: 10.1109/TCSI.2012.2221172.

- [13]. W. Niu, W. Gu and J. Chu, "Experimental investigation of frequency characteristics of underwater wireless power transfer, " 2018 IEEE MTT-S International Wireless Symposium (IWS), 2018, pp.1-3.
- [14]. X. Shi, Q Chang, M Qu, et al. "Effects of coil shapes on wireless power transfer via magnetic resonance coupling," in Journal of Electromagnetic Waves and Applications, vol. 28, no. 11, pp. 1316-1324, 2014.

Weiting Zhang, et. al. "Equivalent mutual inductance model for underwater wireless power transfer." *IOSR Journal of Electrical and Electronics Engineering (IOSR-JEEE)*, 17(2), (2022): pp. 24-33.